BASIC SCIENCE

Nanomedicine: Nanotechnology, Biology, and Medicine
10 (2014) 339–348

Research Article

nanomedjournal.com

Combined mathematical modelling and experimentation to predict polymersome uptake by oral cancer cells

Ian Sorrell, PhD[a], Rebecca J. Shipley, PhD[b], Vanessa Hearnden, PhD[c], Helen E. Colley, PhD[c], Martin H. Thornhill, PhD[c], Craig Murdoch, PhD[c], Steven D. Webb, PhD[a,*]

[a]*Department of Molecular and Clinical Pharmacology, MRC Centre for Drug Safety Science, University of Liverpool, Liverpool, UK*
[b]*Department of Mechanical Engineering, University College London, Torrington Place, London, UK*
[c]*School of Clinical Dentistry, University of Sheffield, Claremont Crescent, Sheffield, UK*

Received 15 May 2013; accepted 29 August 2013

Abstract

This study is motivated by understanding and controlling the key physical properties underlying internalisation of nano drug delivery. We consider the internalisation of specific nanometre size delivery vehicles, comprised of self-assembling amphiphilic block copolymers, called polymersomes that have the potential to specifically deliver anticancer therapeutics to tumour cells. The possible benefits of targeted polymersome drug delivery include reduced off-target toxic effects in healthy tissue and increased drug uptake by diseased tissue. Through a combination of in vitro experimentation and mathematical modelling, we develop a validated model of nanoparticle uptake by cells via the clathrin-mediated endocytotic pathway, incorporating receptor binding, clustering and recycling. The model predicts how the characteristics of receptor targeting, and the size and concentration of polymersomes alter uptake by tumour cells. The number of receptors per cell was identified as being the dominant mechanism accounting for the difference between cell types in polymersome uptake rate.

From the Clinical Editor: This article reports on a validated model developed through a combination of in vitro experimentation and mathematical modeling of nanoparticle uptake by cells via the clathrin-mediated endocytotic pathway. The model incorporates receptor binding, clustering, and recycling and predicts how the characteristics of receptor targeting, the size and concentration alter polymersome uptake by cancer cells.

Key words: Mathematical model; Polymersome; Data fitting; Stochastic model; Endocytosis

Polymersomes are nanometre-sized structures composed of synthetic amphiphilic block copolymers that self-assemble at neutral pH to form enclosed structures. The membranes of polymersomes mimic those formed by natural phospholipids[1,2] and their synthetic nature means that the physical properties, such as membrane thickness and fluidity, can be carefully controlled.[2–4] Consequently, polymersomes exhibit increased stability, elasticity and reduced membrane permeability compared to naturally occurring lipids or liposomes.[5–7] Recently, polymersomes have been developed for the delivery of encapsulated molecules which are rapidly internalised by cells.[8,9] These particular polymersomes are comprised of poly-2-(methacryloyloxy) ethyl phosphorylcholine (PMPC) and poly-2-(diisopropylamino)ethyl methacrylate (PDPA) block copolymers.[10–12] The PDPA block of the copolymer is pH sensitive creating amphiphilic copolymers which self-assemble at pH >6.4 but disassemble when the pH drops below 6.4. Due to their amphiphilic nature, polymersomes can carry different therapeutic loads at the same time. They can encapsulate hydrophilic compounds within their enclosed aqueous core, hydrophobic compounds within their membranes and/or amphiphilic compounds aligned at the hydrophilic-hydrophobic interface.[3–5,13] PMPC–PDPA polymersomes have been shown to be taken up by cells via the endocytotic pathway.[8,14] The dissociation of polymersomes at low pH aids delivery of the encapsulated materials into the cell cytosol as the endosomal pH is typically below 6.4. When the polymersomes enter endosomes

Author contributions: I.S, R.J.S, V.H, H.E.C, M.H.T, C.M and S.D.W designed the research, H.E.C and V.H performed biological experiments, I.S, S.D.W and R.J.S performed mathematical modelling, I.S, C.M and S.D.W wrote the paper.

The authors declare no conflict of interest.

Funding Statement: This work was supported by funding from the Engineering and Physical Sciences Research Council, UK and Yorkshire Cancer Research (5300), UK.

The authors would like to thank Sheila MacNeil for the use of the human derman fibroblasts, Steve Arms, Jeppe Madsen and Adam Blanazs for use of the polymersomes, and Emma Hinsley and Sue Newton for technical assistance.

*Corresponding author: University of Liverpool, Liverpool, UK.
E-mail address: steven.webb@liverpool.ac.uk (S.D. Webb).

1549-9634/$ – see front matter © 2014 Elsevier Inc. All rights reserved.
http://dx.doi.org/10.1016/j.nano.2013.08.013

they rapidly disassemble into individual copolymers, which in turn leads to an osmotic shock which temporarily ruptures the endosomal membrane thus releasing the polymersome–delivered drug into the cytosol, delivering the therapeutic effect.[1,14–16]

Polymersomes are being developed as a treatment tool for a range of disease types. Here, we focus on head and neck squamous cell carcinoma (HNSCC), which includes oral squamous cell carcinoma (OSCC) and is the sixth most common cancer worldwide.[17] Despite improved patient outcomes in a range of cancers, the prognostic implications of HNSCC remain poor. Cisplatin-based chemotherapy and radiotherapy following surgery have become the standard of care, whilst cisplatin in combination with 5-Fluorouracil (5-FU) is the mainstay of treatment for patients with inoperable, recurrent or metastatic disease. Recently, taxanes such as paclitaxel, in combination with cisplatin and 5-FU have been shown to improve survival in patients with locally advanced HNSCC.[18] However, high systemically-delivered doses are required to achieve tumour killing and these lead to myelosuppression, mucositis and significant overall toxicity in patients. Therefore, delivery of anti-cancer drugs directly into the cytosol of tumour cells would significantly reduce off-target toxicity. In support of this, in a murine model[15] it was shown that a single systemic injection of polymersomes dual-loaded with the anti-cancer drugs paclitaxel and doxorubicin caused more tumour cell death, resulted in 50% smaller tumours and had increased drug accumulation with decreased toxicity compared to free drugs alone.[9] Recently, polymersomes have been shown to target tumour cells through their ability to attach ligands or antibodies directed at tumour cell surface receptors, which may reduce off target toxicity further.[19]

To advance new forms of drug delivery it is fundamentally important to understand how the properties of both polymersomes and human cells affect cellular uptake, and how to tune these properties in a treatment-specific way. Here, we develop a mathematical model for polymersome internalisation validated against in vitro studies on polymersome delivery to monolayers of human oral cells and oral tumour cell lines. This model of drug delivery can be applied to other types of cancer cells and other polymer-based delivery systems. Studies into the expression of receptors on the cell surface are combined with the mathematical model to provide crucial insight into the differences in uptake rate between different cell types.

Mathematical models of the endocytosis of nanoparticles as an energy-dependent process dependent on nanoparticle size,[20] receptor-clustering,[21] dose,[22,23] protein corona,[24] and receptor-mediation[25,26] have been studied. To the best of our knowledge, there is no current mathematical model for nanoparticle uptake present in the literature that is time-dependent, encompasses translocation of receptors on the cell surface and includes internalisation rates that depend on receptor-nanoparticle bond number. Our theoretical model incorporates these factors, which proved to be important in validating the model against experimental data. In an extension to the model we include variability in polymersome size to investigate its effect on uptake.

Our mathematical model represents the following critical processes of the cellular uptake of polymersomes: the initial binding of free polymersomes to cell surface receptors; subsequent binding between bound polymersomes and cell receptors; internalisation of polymersomes through endocytosis and the recycling of receptors between the cell interior and surface. In spite of recent developments in the understanding of endocytosis[27] there are still unknowns; for example, the exact role of receptors in the formation of an endosome.[28,29] We test hypotheses on how the number of polymersome-receptor bonds influences uptake by comparing theoretical model output with experimental data.

Methods

Cell culture

This study used the following HNSCC cell lines: Cal27 (American Tissue Culture Collection Manassas, VA, USA), SCC4 (Health Protection Agency Culture Collections, Salisbury, UK) and FaDu (LGC Promochem, Middlesex, UK). Cal27 cells were routinely cultured in Dulbecco's modified Eagle's medium (DMEM), FaDu cells in RPMI-1640 both supplemented with 10% (v/v) fetal calf serum (FCS; BioSera, East Sussex, UK), 2 mM L-Glutamine, 100 IU/ml penicillin and 100 mg/ml streptomycin (Sigma, Poole, UK) and SCC4 in DMEM and Ham's F12 medium in a 1:1 (v/v) ratio supplemented with 10% (v/v) FCS and 5 mg/ml hydrocortisone. Normal oral keratinocytes (NOK) and fibroblasts (NOF) were isolated from biopsies obtained from the buccal and gingival oral mucosa of patients during routine dental procedures with written, informed consent (ethical approval number 09/H1308/66) and cultured as previously described.[19] Human dermal fibroblasts were isolated from skin grafts obtained during routine plastic surgery breast reduction and abdominoplasty operations, with written, informed consent (ethical approval 06/Q2306/25),[30] and cultured in DMEM supplemented with 10% FCS, 2 mM glutamine, 100 IU/ml penicillin and 100 mg/ml streptomycin. All cells were incubated at 37 °C in 5% CO_2 and were sub-cultured after brief treatment with trypsin-EDTA.

Production of rhodamine-labelled polymersomes

$PMPC_{25}$-$PDPA_{70}$ copolymer was synthesized by atom transfer radical polymerization (ATRP) as reported previously.[10,14] To produce rhodamine(rho)-labelled $PMPC_{25}$-$PDPA_{70}$, copolymer was dissolved in a 2:1 chloroform:methanol solution and rho-$PMPC_{30}PDPA_{60}$ (10% v/v) added. The copolymer film was formed by evaporating the solvent overnight in a vacuum oven at 50 °C. The film was rehydrated using 2 ml of 100 mM PBS for 7 days under continuous stirring, sonicated for 15 min and then purified by gel permeation chromatography using a sepharose 4B size exclusion column to extract the fraction containing vesicles of ~200 nm in diameter as determined by dynamic light scattering analysis.[31]

Internalization kinetic analysis using flow cytometry

Full details can be found in the Supplementary Materials. Briefly, rho-PMPC-PDPA polymersomes (0.1 or 1 mg/ml) were added to the cell monolayers and incubated at 37 °C for up to

16 h. Fixed cells were analysed using a FacsArray (BD Biosciences) and the percentage of cells with fluorescence above control cells (cultured in media alone) and median fluorescence of whole cell population measured. Details of the immunoblotting methods and statistical analysis can be found in the Supplementary Materials.

Mathematical model

The mathematical model is a system of $n + 4$ ordinary differential equations, where n is the assumed maximum number of bonds that can form between the polymersome and receptors on a cell surface. The equations below describe how the concentrations of the polymersomes and receptors in different states vary in time. Here, we assume that the concentration of cells is constant (although this could easily be adapted to include cell death, effects of treatment or toxicity) and B_0 denotes the number of free polymersomes per ml in the solution. The rate of change of B_0 over time can be written as

$$\frac{dB_0}{dt} = -k_{3a} n F_s B_0 + k_d B_1, \tag{1}$$

where F_s is the number of free cell surface receptors per ml, B_1 is the number of polymersomes per ml bound to a cell with one bond, k_d is the dissociation rate (per min), and k_{3a} is the binding association parameter[32] for free polymersomes (ml/min). The first term on the RHS of equation (1) represents the binding of a free polymersome to a single receptor. The second term is the dissociation of polymersomes that are bound to only one receptor on the cell surface. The rate at which subsequent bonds form between bound polymersomes and receptors depends on the average number of surface receptors per cell given by F_s/M, where M is the number of cells per ml (assumed constant). The rate equation for B_1 is then given by

$$\frac{dB_1}{dt} = k_{3a} n F_s B_0 - k_d B_1 - \frac{k_{2a}}{M}(n-1) F_s B_1 + 2k_d B_2 - k_{in}(1) B_1, \tag{2}$$

where k_{2a} is the binding association parameter (ml/min) for polymersomes already bound to the surface of a cell and B_2 is the number of polymersomes per ml bound to a cell with two bonds. The function $k_{in}(i)$ gives the internalisation rate (per min) of a polymersome with i bonds (described in more detail below). The third term on the RHS of equation (2) is the rate at which polymersomes bound to one receptor subsequently bind to another receptor on the same cell. The fourth term is the rate that polymersomes bound by two bonds revert to being bound by a single bond through the dissociation of one bond (the dissociation rate is double that of equation (1) as there are double the number of bonds that can dissociate). Generalizing this to number of polymersomes per ml with i bonds, B_i, yields

$$\frac{dB_i}{dt} = \frac{k_{2a}}{M}(n-i+1) F_s B_{i-1} - i k_d B_i - \frac{k_{2a}}{M}(n-i) F_s B_i + (i+1) k_d B_{i+1} - k_{in}(i) B_i, \tag{3}$$

for $i = 2,\ldots,n\text{-}1$. The equation for the number of polymersomes per ml with the maximum number n bonds, B_n, is given by

$$\frac{dB_n}{dt} = \frac{k_{2a}}{M} F_s B_{n-1} - n k_d B_n - k_{in}(n) B_n. \tag{4}$$

The equations for the rate of change of the number per ml of free (unbound) surface and internalised receptors, F_s and F_{in} respectively, are given by

$$\frac{dF_s}{dt} = -k_{3a} n F_s B_0 - \frac{k_{2a}}{M} F_s \sum_{i=1}^{n-1} (n-1) B_i + k_d \sum_{i=1}^{n} i B_i + r F_{in}, \tag{5}$$

$$\frac{dF_{in}}{dt} = \sum_{i=1}^{n} i k_{in}(i) B_i - r F_{in}, \tag{6}$$

where r is the rate at which internalised receptors are recycled back to the cell surface. Finally, the equation for the rate of change of internalised polymersomes B_{in} is given by

$$\frac{dB_{in}}{dt} = \sum_{i=1}^{n} k_{in}(i) B_i. \tag{7}$$

The internalisation rate of a polymersome may depend on the number of receptors bound to it as receptor clustering can promote clathrin-coated pit initiation.[29] To test this we used two internalisation functions: the saturating function $k_{in}(i) = k_{in}^{i\gamma}/(i_*^{\gamma} + i^{\gamma})$, where γ and i_* are parameters controlling the slope and the threshold of the function respectively and there is dependence on bond number i; and the constant function, $k_{in}(i) = k_{in}$, which is independent of bond number.

For the most part, the ODE model above is used in the analysis. However, to validate the model against the experimental data for the percentage of cells positive for polymersomes as a function of time (Figure 1, *A*), the mathematical model is converted to a stochastic model accounting for individual cells and individual polymersomes using a Monte Carlo simulation (Gillespie Algorithm,[33] see Supplementary Materials). Variability in the cell receptor number and polymersome size is also included in the stochastic model to investigate how changes in the polymersome properties (e.g. size) or cell characteristics (e.g. receptor number) alter the model predictions. We include this variability in the model by assuming distributions of the relevant model parameters (see Supplementary Materials).

Model parameters and initial conditions

The experimental concentration of polymersomes in mg/ml is converted to number per ml for the mathematical model using the number of copolymers per polymersome and the molecular mass of a copolymer chain. A 100 nm polymersome is composed of 400 copolymer chains.[8] The number average molecular weight of $PMPC_{25}$-$PDPA_{70}$ is 22000 g/mol.[34] Therefore, a polymersome concentration of 1 mg/ml is equivalent to 6.81×10^{13} polymersomes/ml. The concentration of cells in the uptake studies was 5×10^4 cells/ml. The initial concentration of receptors is determined from fitting the model to the available

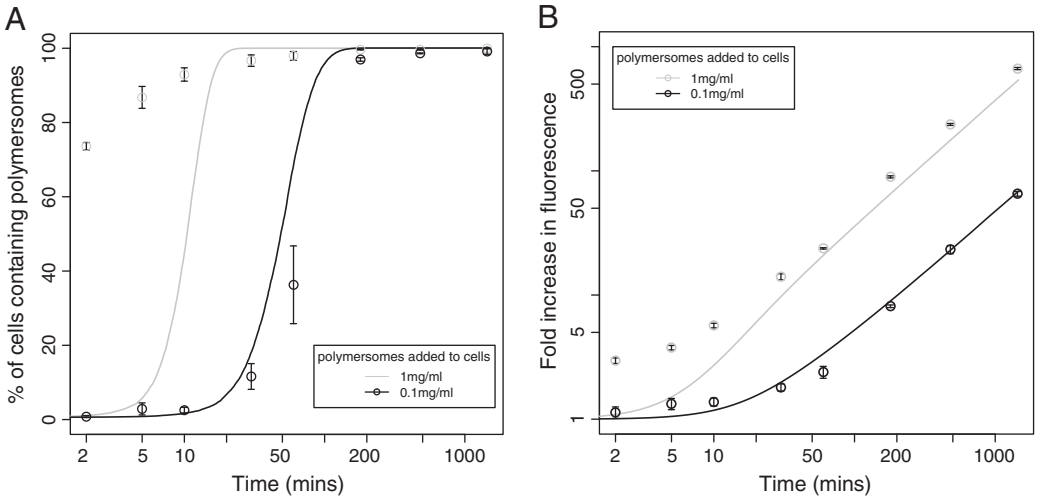

Figure 1. Uptake of polymersomes at two concentrations (0.1 and 1 mg/ml) in FaDu cells and fitted mathematical model output. Percentage of population positive for polymersomes **(A)** and fold increase in fluorescence compared to control **(B)**. Model parameters $k_{3a} = 1.4 \times 10^{-19}$, $k_{2a} = 3.9 \times 10^{-3}$, $k_{in} = 0.612$, $n = 40$, $r = 0.1$, $k_d = 3.75 \times 10^{-25}$, $\gamma = 1$ and $i_* = 7$.

data. The predicted number of receptors per cell was compared to typical numbers of receptors per cell[32] to ensure physically meaningful quantities. The other parameters estimated by fitting are the binding rates k_{3a} and k_{2a}, the maximum number of receptor-polymersome bonds n and the dissociation rate k_d. In most cases the saturating internalisation function was used with parameters γ and i_* also estimated by fitting. The internalisation rate k_{in} was taken to be 0.612 per min[21] unless stated otherwise. The receptor recycling rate was chosen to be 0.1 per min, as receptors are recycled back to the plasma membrane within minutes[27] and the model predictions turn out not to be sensitive enough to the recycling rate for it to be fitted to the data. The method of solution for the model is described in the Supplementary Materials along with details of the fitting process. A list of the parameter values is shown in Table 1.

Results

Concentration-dependent study

Figure 1, *A* and *B* show the experimental data for the uptake of PMPC-PDPA polymersomes by FaDu cells at 1 and 0.1 mg/ml, and the corresponding mathematical model output. The percentage of cells containing a detectable amount of polymersomes (Figure 1, *A*) is significantly ($P < 0.05$) higher for cells exposed to 1.0 compared to 0.1 mg/ml rho-labelled polymersomes for up to 100 min. The fold increase in the median fluorescence intensity was also significantly higher when the cells were exposed to a higher concentration of polymersomes (Figure 1, *B*). This study determined the following mathematical model parameters: number of receptors per FaDu cell; binding rates k_{3a} and k_{2a}, dissociation rate k_d and parameters γ and i_*. Although the fit is reasonable for both doses at later time points (>10 min), where the average percentage error is 23% for the high dose and 13% for the low dose, there are large relative errors (>50%) between the high dose data and simulation at early time points (≤10 min). Sets of parameters that produce predictions for the high dose data that match the early time points had large residual errors at later time points even when the fitting process was applied to the high dose data alone (the results shown are for fitting to both doses simultaneously). The inability of the model to fit to early and late time points of the high dose data may be due to cellular adaptive responses which slow the initially rapid uptake, or there may be another limiting process that is quickly saturated at high doses. The curves for the simulations of percentage of cells containing polymersomes are expected to be steeper than the experimental data because of the lack of variability in the simulated cells. Note the saturating internalisation function $k_{in}(i)$ was used, with parameters $\gamma = 1$ and $i_* = 7$.

Effect of cell type on polymersome uptake

Figure 2, *A* and *B* show the experimental data for polymersome uptake for six cell types; two OSCC (Cal27, SCC4), one oropharyngeal (FaDu) cell line and three primary cell types; normal human oral keratinocytes (NOK), normal oral fibroblasts (NOF) and human dermal fibroblasts (HDF). The carcinoma cell lines show a significantly ($P < 0.05$) higher percentage of cells containing polymersomes (Figure 2, *A*) and display increased fluorescence demonstrating a higher rate of polymersome up-take than NOK, NOF or HDF up to 100 min (Figure 2, *B*). Figure 2, *C* and *D* show the output from model simulations. The different lines are reproduced by varying receptor number for each cell line. The similarity between the experimental data and model output suggests that differences in uptake rates between cell types can be explained by differences in the numbers of polymersome binding receptors on the cells. The parameters used were those determined by the concentration-dependent study and the saturating internalisation function was used.

Fitting to data from different cell types gives predictions for the number of receptors per cell. The predicted number will depend on other parameters, such as binding and internalisation

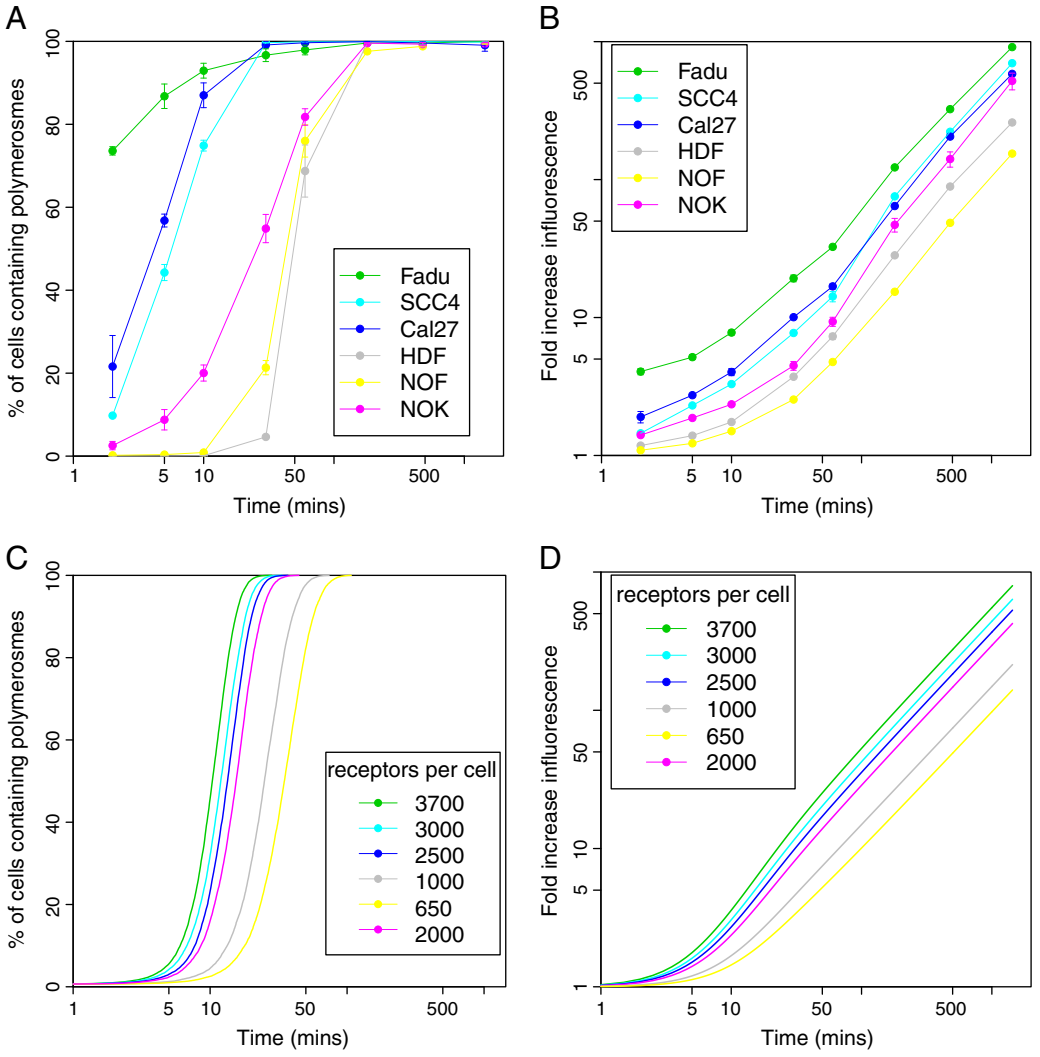

Figure 2. Uptake of polymersomes by monolayers of various cell types **(A, B)** and mathematical model output **(C, D)** for cells with various numbers of receptors. Percentage of population positive for polymersomes **(A, C)** and fold increase in fluorescence compared to control **(B, D)**. Model parameters k_{3a} = 1.4×10^{-19}, $k_{2a} = 3.9 \times 10^{-3}$, $k_{in} = 0.612$, $n = 40$, $r = 0.1$, $k_d = 3.75 \times 10^{-25}$, $\gamma = 1$ and $i_* = 7$.

Table 1
Parameters in the mathematical model.

Parameter (unit)	Notation	Value
Binding association rate free polymersomes to receptors (ml/min)	k_{3a}	1.4×10^{-19}
Binding association rate bound polymersomes to receptors (ml/min)	k_{2a}	1.9×10^{-3}
Internalisation rate (min^{-1})	k_{in}	0.612
Dissociation rate (min^{-1})	k_d	3.7×10^{-5}
Maximum number polymersome:receptor bonds (dimensionless)	n	40
Internalisation saturating function (dimensionless)	γ, i_*	1, 7
Receptor recycling rate (min^{-1})	r	0.1

rates, and the form of internalisation function. This is illustrated in Figure 3 which shows how predictions for receptor number depend on the internalisation function and the other model parameters. To make predictions on receptor number the model is fitted to the data on fold increase in fluorescence (Figure 2, *B*). The predictions are for the two cell types (NOF and FaDu) where the receptor expression has been measured. Figure 3, *A* and *B* show the percentage difference in the number of receptors per cell that best fit the NOF and FaDu data for different combinations of the binding rates k_{3a} and k_{2a}. The figure includes the ranges of k_{3a} and k_{2a} that can produce predictions (depending on the other parameters) within 5% of the experimental data at times greater than 50 min. In Figure 3, *A* the internalisation function used was saturating, whereas in

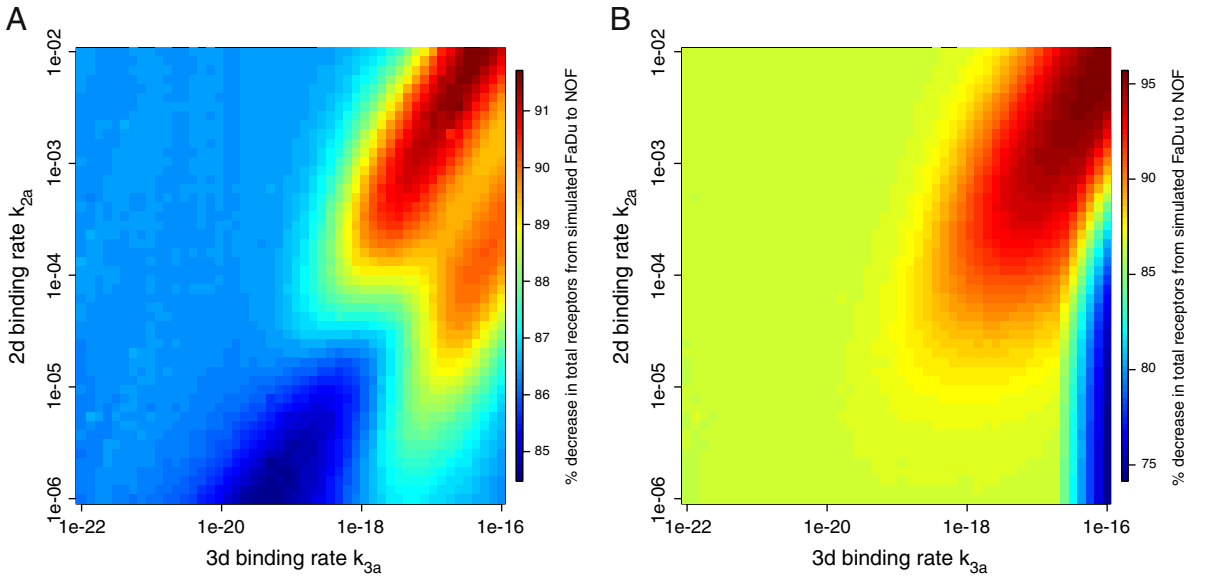

Figure 3. Mathematical model predictions for the difference in number of receptors per cell between FaDu and NOF cells given as the percentage decrease when comparing NOF to FaDu for a range of values of the binding parameters k_{2a} and k_{3a}. In **(A)** the internalisation function used was saturating. In **(B)** the internalisation function used was a constant. The other parameters were $k_{in} = 0.612$, $n = 40$, $r = 0.1$, $k_d = 3.75 \times 10^{-25}$, $\gamma = 1$ and $i_* = 7$.

Figure 3, *B* the internalisation function was constant. For both types of internalisation function at least 85% reduction in receptor number is predicted between FaDu and NOF cells for nearly all values of k_{3a} and k_{2a} considered.

Of course, differences in the cells, other than receptor number, may also explain the differences in uptake rate. However, we do not consider differences in binding rates k_{3a} and k_{2a} between cell types. These are determined by the diffusion of polymersomes and interactions between polymersomes and the cell membrane. We assume that these factors are roughly similar across cell types; however, the rate of endocytosis may vary between cell types and influence uptake. Consider the simplest case that polymersome internalisation is independent of bond number and the only difference between cell types is the constant rate of internalisation k_{in}. In this case, to match the observed differences in uptake the model predicted unrealistic values for the internalisation rate k_{in} of either NOF or FaDu cells. Depending on the binding rates k_{3a} and k_{2a} the model predicted FaDu cells would have to uptake polymersomes at a rate exceeding plausible rates of endocytosis (considering the observed lifetime and quantity of clathrin-coated pits[29]), or NOF cells would have a rate of endocytosis at least three orders of magnitude slower than FaDu cells. This suggests that a difference in the rate of endocytosis between NOF and FaDu cells is unlikely by itself to account for the difference in their uptake rates.

To experimentally test whether receptor numbers can explain differences in uptake between cell types, the receptors involved in polymersome binding were determined and their expression by cell type quantified. Recent data suggest that the receptors likely to be involved in binding polymersomes belong to the scavenger receptor class B family.[18] Immunoblotting shows that FaDu expresses 5 fold more scavenger receptor class BI/BII than NOF (Figure 4).

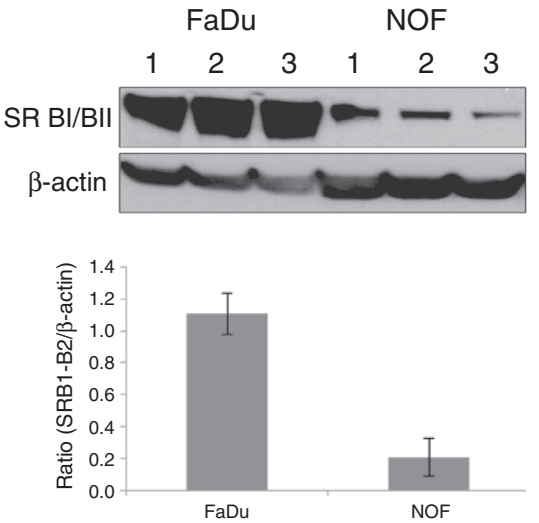

Figure 4. Cell lysates were separated by SDS-PAGE and immunoblotted for Scavenger receptor BI + BII and β-actin (as a loading control). A representative blot is shown for SRBI + SRBII and the intensity of the band determined by densitometry and normalised to β-actin levels in the same sample.

Polymersome size variability

Although the model does not include size of the polymersome explicitly as a parameter, model parameters implicitly depend on it. For example, larger polymersomes will diffuse slower but may bind faster to cell surface receptors. Both effects will alter binding rates. Larger polymersomes will also have a larger maximum bond number n and may need more bonds before they are internalised, which is

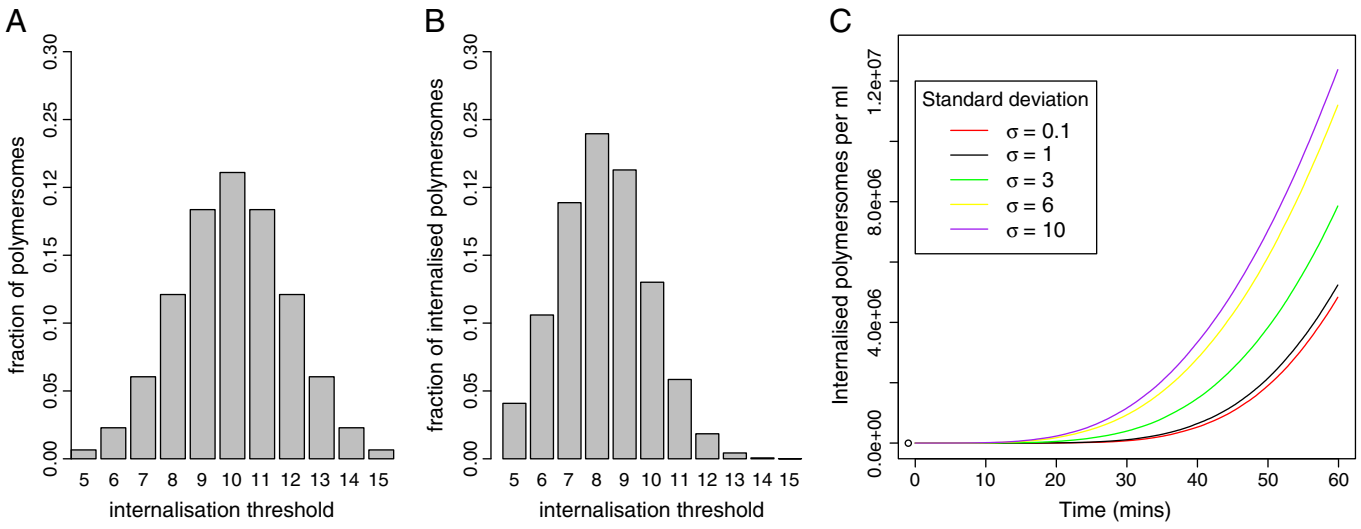

Figure 5. Distribution of internalisation threshold for free polymersomes **(A)** used in mathematical model resulting in distribution of internalised polymersomes **(B)**. Uptake of polymersomes **(C)** for various standard deviations σ of the distribution of the internalisation threshold of the free polymersomes. Model parameters $k_{3a} = 1.4 \times 10^{-19}$, $k_{2a} = 3.9 \times 10^{-3}$, $k_{in} = 0.612$, $n = 40$, $r = 0.1$, $k_d = 3.75 \times 10^{-25}$, $\gamma = 1$ and mean $i_* = 10$.

represented by a larger threshold in the saturating internalisation function. Controlling the size of polymersomes is part of the experimental design but the success of this process is often limited; instead there is typically a Gaussian distribution of polymersome sizes present in any real sample. To investigate how this variability affects the uptake of polymersomes, a distribution of polymersomes can be included in the stochastic model through a discrete distribution in one of the relevant parameters. For more details see the Supplementary Materials.

The distribution in Figure 5, *A* represents polymersomes that vary in their internalisation threshold by up to 50% as larger polymersomes may require more receptor ligand bonds before they are internalised. Figure 5, *A* shows the distribution of free polymersomes added to the cells whilst Figure 5, *B* shows the distribution of internalised polymersomes. The mean threshold number, which should be positively correlated to size, is lower for the internalised polymersomes. Therefore, if these polymersomes carried a therapeutic load, the amount of drug delivered per cell would be lower than expected from the number of polymersomes internalised per cell and the mean amount of drug carried. However, Figure 5, *C* shows the uptake of polymersomes increases as the standard deviation of the size of the free polymersomes increases. This is because the rate a polymersome progresses from initial binding to internalisation will depend on the reciprocal of the threshold number of bonds. Polymersomes with a threshold of $i_* = 5$, for example, will be internalised at roughly twice the rate of the median sized ($i_* = 10$) polymersomes, whereas polymersomes with a threshold of $i_* = 15$ will be internalised at roughly 75% of the rate of the median. In the simulations the increase in the number of 'smaller' polymersomes more than compensates for the increase in the number of 'larger' polymersomes and results in an increased rate of total uptake.

For a constant internalisation function, a distribution of values of the rate k_{in} is one way to capture variations in internalisation due to polymersome size. However, varying the standard deviation of this distribution had almost no effect on the overall polymersome uptake rate. The distribution of internalised polymersomes was almost identical to the distribution of free polymersomes (data not shown).

Larger polymersomes will have more binding sites and may bind to more receptors faster. This will then decrease the number of receptors available for binding to other polymersomes. Note that if the polymersomes were coated in targeting ligands this would correspond to the number of ligands per polymersome. The distributions in Figure 6 represent free (Figure 6, *A*) and internalised (Figure 6, *B*) polymersomes that differ in their number of binding sites n. In this case, the mean of the distribution of internalised polymersomes is higher than the mean for the free polymersomes. Figure 6, *C* shows how the standard deviation of the polymersome distribution affects uptake rates. Again, a wider distribution increases the uptake rate.

Discussion

This study provides insight into the interaction between polymersomes and cells in order to aid the design of drug carriers and treatment regimes. Theoretical models were used to test assumptions on cellular processes to identify the important factors for further experimentation that will, in turn, lead to improved theoretical models. Our theoretical model could be applied to other nanoparticles and cell types where the uptake mechanism is clathrin-mediated endocytosis, with suitable experimental data required to appropriately parameterize the model.

The mathematical model is parameterized against experimental data for two concentrations of polymersomes administered to cell monolayers. Importantly, this makes it is possible to

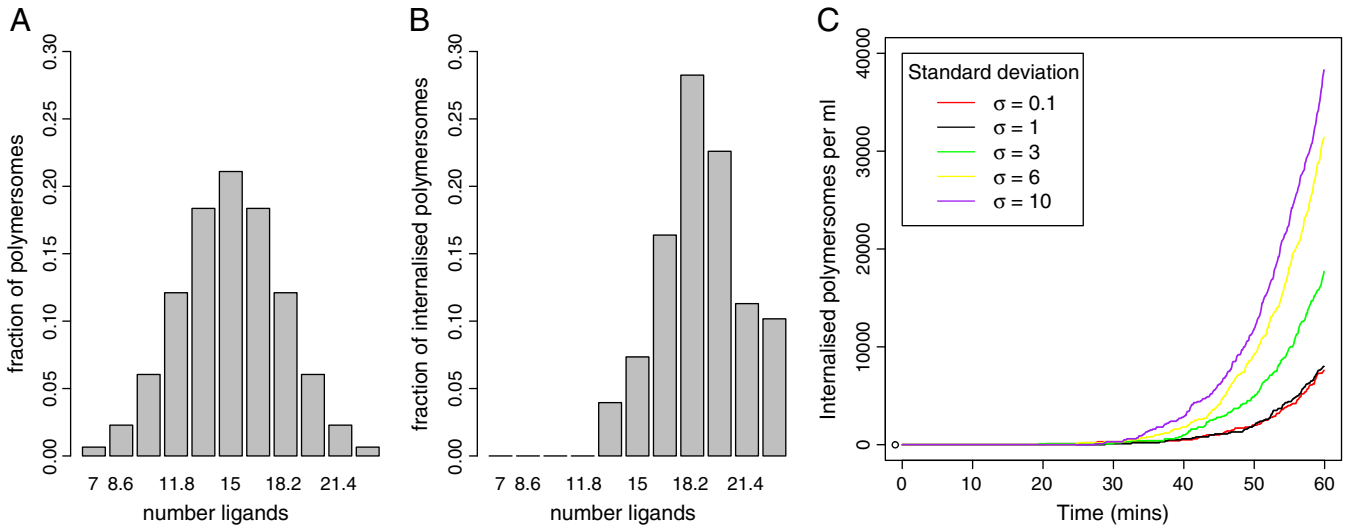

Figure 6. Distribution of number of binding sites for free polymersomes **(A)** used in mathematical model resulting in distribution of internalised polymersomes **(B)**. Uptake of polymersomes **(C)** for various standard deviations σ of the distribution of the binding sites of the free polymersomes. Model parameters $k_{3a} = 1.4 \times 10^{-19}$, $k_{2a} = 3.9 \times 10^{-3}$, $k_{in} = 0.612$, mean $n = 15$, $r = 0.1$, $k_d = 3.75 \times 10^{-25}$, $\gamma = 1$ and $i_* = 5$.

estimate the intracellular drug concentration after a known administered concentration. The mathematical model was used to test hypotheses on the different cellular mechanisms involved in the uptake of the polymersomes. The role of receptors in the uptake of polymersomes (and other nanoparticles) is not fully understood.[28] We look at two possibilities; that either the rate of internalisation of a polymersome bound to the surface of the cell is dependent or independent of the number of receptors it is bound to. In the model these possibilities are represented by an internalisation function that was either constant or a saturating function of the number of receptor-polymersome bonds (other functions could have been used but any dependency is likely to be saturating – since the process is receptor mediated). A steep sloped saturating function approximates a threshold effect, which represents the number of receptor-polymersome bonds that are needed before internalisation occurs. We found that the mathematical model matched the data better when the internalisation function was saturating rather than constant. This could be due to the two extra unknown parameters that are fitted; however, the difference between the two suggests that the saturating function is more appropriate inferring the rate of uptake of polymersomes is dependent on the number of bonds and a threshold effect may be in operation.

Understanding the variation in polymersome uptake across different cell types is important in the potential use of polymersomes as an anti-cancer drug delivery system. Targeted delivery of drugs to cancer cells with delivery vehicles is highly desired as it could result in less off-target side effects and higher cancer cell killing efficiency. Although this study did not use polymersomes with attached ligands there was still a significantly higher uptake of polymersomes into cancer cell lines compared to primary cells. The difference between cell types was investigated using the mathematical model. Figure 2, *C* and *D* show how altering the receptor number changes the uptake of polymersomes in line with the observed experimental uptake rates in the different cell lines, suggesting that receptor number could be responsible for differences in cellular uptake between different cell types. Recent data obtained by us and others suggest that type B scavenger receptors are likely to be involved in the endocytosis of polymersomes.[18] We found that FaDu expressed significantly more SRB1-B2 than NOF. We fitted the mathematical model to the FaDu and NOF receptor data and found that the model predicts FaDu cells have typically at least 85% more receptors that bind to polymersomes than NOF. This was broadly in agreement with the experiments (Figure 4) and indicated that receptor number has a dominant effect on the differences in uptake between these two cell types. Scavenger receptors are expressed in large quantities on macrophages. This corresponds to results from an *in vivo* murine cancer model where polymersomes accumulated in macrophages.[31]

Although the polymersomes are controlled for size, there will still be a distribution of sizes in any sample of manufactured polymersomes. This could affect the uptake of polymersomes, so we assessed the importance of reducing the standard deviation of the polymersome size distribution. The mathematical model does not explicitly include polymersome size, but several of the model parameters will depend implicitly on it.[14] Therefore we used the stochastic model with non-identical polymersomes represented by parameter distributions. If the internalisation function was constant, a distribution in the internalisation rate k_{in} did not alter the uptake of polymersomes and the distributions of free and internalised polymersomes were identical. If the internalisation function was saturating, then distributions in the internalisation threshold and the number of binding sites n both showed an increased uptake with increasing standard deviation. Also the mean size of the polymersome internalised differed from the mean size of the free polymersomes. The distributions used here should be considered as distributions of polymersomes around

200 nm, the size of polymersomes used in this study. Much smaller or larger polymersomes will be affected by other physical aspects of endocytosis. For example, a reduction in gold nanoparticle uptake by HeLa cells below approximately 40 nm and above 50 nm has been reported.[35] In our model the reduced uptake below 40 nm could correspond to the internalisation rate being a threshold effect where a minimum number of receptor-polymersome bonds are needed before internalisation. Nanoparticles smaller than the threshold might not bind to enough receptors for internalisation to be completed. The amount of therapeutic load the cells are exposed to will depend on the size and number of the polymersomes. Given experimental data on the dependency of polymersome size on uptake,[14] the relationships between size and the model parameters could be estimated. From this, the model can predict the optimum size of polymersomes to be used in treatment and how much the variability in size of a sample of polymersomes will alter the uptake and encapsulated drug delivery.

In the mathematical model, receptors are recycled to the surface at a fixed rate. Regulation of receptor recycling and production probably occurs biologically and may depend on the number of internalised polymersomes. However, the model achieves a good fit to the experimental data so regulation of receptors may not be an important factor for the polymersomes and receptors considered here. However it is considered to be a factor in the uptake of other nanoparticles[21] and will feature in our ongoing work on this model.

Appendix A. Supplementary data

Supplementary data to this article can be found online at http://dx.doi.org/10.1016/j.nano.2013.08.013.

References

1. Disher DE, Ahmed F. Polymersomes. *Annu Rev Biomed Eng* 2006;**8**:323-41.
2. Disher DE, Eisenberg A. Polymer vesicles. *Science* 2002;**297**:967-73.
3. Battaglia G, Ryan AJ, Tomas S. Polymeric vesicle permeability: a facile chemical assay. *Langmuir* 2006;**22**:4910-3.
4. Graff A, Sauer M, Van Gelder P, Meier W. Virus-assisted loading of polymer nanocontainer. *Proc Natl Acad Sci USA* 2002;**99**:5064-8.
5. Battaglia G, Ryan AJ. Bilayers and interdigitation in block copolymer vesicles. *J Am Chem Soc* 2005;**127**:8757-64.
6. Discher BM, Won YY, Ege DS, et al. Polymersomes: Tough vesicles made from diblock copolymers. *Science* 1999;**284**:1143-6.
7. Bermudez H, Brannan AK, Hammer DA, Bates FS, Discher DE. Molecular weight dependence of polymersome membrane structure, elasticity, and stability. *Macromolecules* 2002;**35**:8203-8.
8. Lomas H, Massignani M, Abdullah KA, et al. Non-cytotoxic polymer vesicles for rapid and efficient intracellular delivery. *Faraday Discuss* 2008;**139**:143-59 [discussion 213-28, 419-20].
9. Ahmed F, Pakunlu RI, Brannan A, Bates F, Minko T, Discher DE. Biodegradable polymersomes loaded with both paclitaxel and doxorubicin permeate and shrink tumors, inducing apoptosis in proportion to accumulated drug. *J Control Release* 2006;**116**:150-8.
10. Du J, Tang Y, Lewis AL, Armes SP. pH-sensitive vesicles based on a biocompatible zwitterionic diblock copolymer. *J Am Chem Soc* 2005;**127**:17982-3.
11. Shen L, Du J, Armes SP, Liu S. Kinetics of pH-Induced formation and dissociation of polymeric vesicles assembled from a water-soluble zwitterionic diblock copolymer. *Langmuir* 2008;**24**:10019-25.
12. Giacomelli C, Le Men L, Borsali R, et al. Phosphorylcholine-based pH-responsive diblock copolymer micelles as drug delivery vehicles: light scattering, electron microscopy, and fluorescence experiments. *Biomacromolecules* 2006;**7**:817-28.
13. Ghoroghchian PP, Frail PR, Susumu K, et al. Near-infrared-emissive polymersomes: self-assembled soft matter for in vivo optical imaging. *Proc Natl Acad Sci USA* 2005;**102**:2922-7.
14. Massignani M, LoPresti C, Blanazs A, et al. Controlling cellular uptake by surface chemistry, size, and surface topology at the nanoscale. *Small* 2009;**5**:2424-32.
15. Ahmed F, Pakunlu RI, Srinivas G, et al. Shrinkage of a rapidly growing tumor by drug-loaded polymersomes: pH-triggered release through copolymer degradation. *Mol Pharm* 2006;**3**:340-50.
16. Lomas H, Canton I, MacNeil S, et al. Biomimetic pH sensitive polymersomes for efficient DNA encapsulation and delivery. *Adv Mater* 2007;**19**:4238-43.
17. Argiris A, Karamouzis MV, Raben D, Ferris RL. Head and neck cancer. *Lancet* 2008;**371**:1695-709.
18. Specenier P, Vermorken JB. The role of taxanes and targeted therapies in locally advanced head and neck cancer. *Curr Opin Oncol* 2007;**19**:195-201.
19. Lee JS, Groothuis T, Cusan C, Mink D, Feijen J. Lysosomally cleavable peptide-containing polymersomes modified with anti-EGFR antibody for systemic cancer chemotherapy. *Biomaterials* 2011;**32**:9144-53.
20. Chaudhuri A, Battaglia G, Golestanian R. The effect of interactions on the cellular uptake of nanoparticles. *Phys Biol* 2011;**8**:046002.
21. Ghaghada KB, Saul J, Natarajan JV, Bellamkonda RV, Annapragada AV. Folate targeting of drug carriers: a mathematical model. *J Control Release* 2005;**104**:113-28.
22. Salvati A, Aberg C, dos Santos T, et al. Experimental and theoretical comparison of intracellular import of polymeric nanoparticles and small molecules: toward models of uptake kinetics. *Nanomedicine* 2011;**7**:818-26.
23. Mukherjee SP, Byrne HJ. Polyamidoamine dendrimer nanoparticle cytotoxicity, oxidative stress, caspase activation and inflammatory response: experimental observation and numerical simulation. *Nanomedicine* 2013;**9**:202-11.
24. Dell'Orco D, Lundqvist M, Cedervall T, Linse S. Delivery success rate of engineered nanoparticles in the presence of the protein corona: a systems-level screening. *Nanomedicine* 2012;**8**:1271-81.
25. Alarcón T, Page KM. Mathematical modeling of the VEGF receptor. In: Jackson TL, editor. *Modeling tumor vasculature*. New York: Springer; 2012. p. 3-35.
26. Gexfabry M, Delisi C. Receptor-Mediated Endocytosis – a Model and Its Implications for Experimental-Analysis. *Am J Physiol* 1984;**247**:R768-79.
27. McMahon HT, Bourcot E. Molecular mechanism and physiologival functions of clathrin-mediated endocytosis. *Nat Rev Mol Cell Biol* 2011;**12**:517-33.
28. Santini F, Keen JH. Endocytosis of activated receptors and clathrin-coated pit formation: deciphering the chicken or egg relationship. *J Cell Biol* 1996;**132**:1025-36.
29. Liu AP, Aguet F, Danuser G, Schmid SL. Local clustering of transferrin receptors promotes clathrin-coated pit initiation. *J Cell Biol* 2010;**191**:1381-93.
30. Smith LE, Hearnden V, Lu Z, et al. Evaluating the use of optical coherence tomography for the detection of epithelial cancers in vitro. *J Biomed Opt* 2011;**16**:116015.
31. Murdoch C, Reeves KJ, Hearnden V, et al. Internalization and biodistribution of polymersomes into oral squamous cell carcinoma cells in vitro and in vivo. *Nanomedicine* 2010;**5**:1025-36.

32. Lauffenburger DA, Linderman JJ. *Receptors: Models for Binding*. Trafficking and Signalling: Oxford University Press; 1996.
33. Imamura M, Kumagai T, Sugihara N, Furuno K. High-performance liquid chromatographic assay of 3′-phosphoadenosine 5′-phosphosulfate (PAPS) and UDP-glucuronic acid (UDPGA) in cultured hepatic cell extracts. *J Health Sci* 2003;**49**:395-400.
34. Lomas H, Du J, Canton I, et al. Efficient encapsulation of plasmid DNA in pH-sensitive PMPC-PDPA polymersomes: study of the effect of PDPA block length on copolymer-DNA binding affinity. *Macromol Biosci* 2010;**10**:513-30.
35. Chithrani BD, Chan WC. Elucidating the mechanism of cellular uptake and removal of protein-coated gold nanoparticles of different sizes and shapes. *Nano Lett* 2007;**7**:1542-50.